Tellus (1990), *42A*, 343–365

On the operational predictability of blocking

By STEFANO TIBALDI* and FRANCO MOLTENI, *European Centre for Medium-range Weather Forecasts, Reading, UK*

(Manuscript received 31 May 1988; in final form 29 March 1989)

ABSTRACT

The entire 7-year archive of ECMWF operational analysis and forecast data is used to assess the skill of the Centre's model in short- and medium-range forecasting of atmospheric blocking. The assessment covers 7 100-day periods, from 1 December to 10 March of all winters from 1980–81 to 1986–87, inclusive. A slightly modified version of the Legenäs and Økland objective zonal index is used to quantify both observed and forecast occurrence of blocking. The study is performed on 500 hPa geopotential height and on Euro-Atlantic and Pacific blocking separately. It is found that blocking frequency is severely underestimated in medium-range forecasts; the model is, on average, reasonably skilful if the initial conditions are blocked, but blocking onset is poorly represented if it occurs more than a few days into the forecast. This inability in entering the blocking regime has a substantial impact on the systematic error of the model.

1. Introduction

Atmospheric blocking has long been recognized as a physical process of profound dynamical interest and of great practical relevance to operational forecasting. The crucial role that the onset, development and decay of block-like structures have on atmospheric low-frequency variability, and therefore on short-, medium- and long-range forecasting, has made blocking one of the most studied atmospheric processes. For a review of recent observational, theoretical and numerical work on blocking, the reader is referred to Hollingsworth et al. (1987) and to Benzi et al. (1986c).

Regarding the ability of numerical models to represent blocking, a few studies have been performed on long model integrations in order to assess the incidence of blocking in comparison with observed frequencies, duration and preferred locations, e.g., Mansfield (1984), Lau (1983). In order to perform such comparisons, the observational studies of Rex (1950), Dole and Gordon (1983), Lejenäs and Økland (1983) and others have been used. Actual deterministic forecasting of blocking from observed initial conditions (as it is done in a routine numerical weather forecasting environment) has so far been even less documented, essentially because of the lack of a large homogeneous database of operational forecasts. Despite this lack of objective assessments of forecasting models' skill in representing blocking, there seems to be some sort of consensus among both modellers and synopticians on the fact that models perform slightly better during, and in the areas of, blocking than in situations of prevailing zonal flow (e.g., A. Persson, personal communication), but then persistence does the same, alas. Such feelings have also been quantified by synoptic evaluation of model performance during some individual blocking cases (see Bengtsson, 1981; Grønaas, 1982; Tibaldi and Ji, 1983; Ji and Tibaldi, 1983).

The European Centre for Medium-Range Weather Forecasts (ECMWF) has now been producing and archiving operational analyses and medium-range forecasts for more than 7 years; these archives make it now possible to try to quantify in a more objective way the ability of

* Current address: Universita' di Bologna, Dipartimento di Fisica, Via Irnerio 46, 40126 Bologna, Italy.

a state-of-the-art global forecasting model in representing blocking onset and maintenance. This is the purpose of this work. Section 2 describes, first of all, the database used for this study and the objective index that is used to determine whether or not a given analysis (or forecast) is considered to be blocked at a given longitude. Section 3 gives an account of the overall model performance in representing blocking as a function of longitude and in different years. Section 4 deals with the separate diagnosis of Euro-Atlantic and Pacific blocking, while Section 5 concentrates on blocking onset and blocking maintenance. Section 6 is devoted to the diagnosis of the model systematic error during different flow regimes and Section 7 gives a summary and attempts to draw some conclusions.

2. The database and the definition of an objective blocking index

The database for this study is composed of all day 1 to 10 forecasts (and verifying analyses) of 500 hPa geopotential height valid from 1 December to 10 March, from 1980–81 to 1986–87 inclusive. Although each of the 7 100-day periods does not correspond exactly to the astronomical winter, we will refer to them as seven "winter" periods. All day 1 to 10 forecasts verify on the date of the corresponding analysis and are, therefore, initiated from different initial conditions (progressively lagging in time), in a way paralleling exactly the dataset used by Lorenz in his 1982 study (Lorenz, 1982). The complete dataset is therefore composed of 7700 fields (11 forecast times, including analysis time, 100 days per winter, 7 winter periods) projected on spherical harmonic coefficients truncated at triangular truncation 40 (T40). Although the original fields are global, we will restrict our analysis to the middle latitudes of the Northern Hemisphere, for which independent observational studies of blocking frequency on much larger datasets are available for the sake of comparison. One of the main limitations of this work (but by no means the only one) is due to the fact that the analysis was only carried out for a single season and at a single vertical level (500 hPa). This is due to a variety of practical reasons, almost all having invariably to do with the amount of data to unload from the operational archives and to process further. There are plans to extend such analysis firstly to other periods of the year and then to other levels (and perhaps to the other hemisphere as well). Another important limitation of our work is connected to the fact that the operational ECMWF General Circulation Model (GCM) has undergone several changes during the period here considered, many of which of major importance, be they of numerical nature (grid-point versus spectral technique or horizontal and vertical resolution) or of physical nature (parameterization of moist convection, vertical and horizontal diffusion and orographic effects). This limitation cannot be practically avoided if we want to have at our disposal a dataset of considerable size. Had we limited ourselves to a single period during which the model has been subject to only minor modifications, the statistical significance of our results (already very limited with a total dataset composed of 700 days) would have been negligible.

In any objective study of atmospheric blocking, one of the main difficulties is to devise an objective method to determine whether a given flow pattern is blocked or not at a certain point (or over a certain area) at a given moment in time (or over a certain period of time). This is related to the fact that no such thing as a typical block exists and the Earth's atmosphere uses very many of its almost infinite degrees of freedom to realize a variety of "similar" but in fact quite diverse situations, all of them in some sense blocked. It is therefore extremely difficult to define a method that will satisfy the personal criteria of any number (however small but greater than one) of experienced synopticians. This work is no exception to this rule but, in addition to the usual disclaimers, we would like to point out that our main goal is not to diagnose the statistics of observed blocking in its spatial and temporal details, but to compare analysed and forecast fields, after having projected them on a suitable indicator. We hope that many of the shortcomings and limitations of our choice of objective definition of blocking will be of little relevance when the indicator is used in this "comparison mode". We will try to point out those results that might be most affected by the particular nature of the indicator.

We will, first of all, give here a local and instantaneous definition of blocking and later, in Section 4, generalize this to take into account longitudinal extension and time duration. This definition is essentially derived from the work of Lejenäs and Økland (1983) to which the reader is referred for a more extensive justification of the criteria, not dissimilar to those used by Rex (1950). The procedure we have applied is as follows: the 500 hPa field is firstly evaluated on a 4° by 4° regular latitude-longitude grid covering the Northern Hemisphere. Then the geopotential height gradients GHGS and GHGN (referring to middle and high latitudes respectively) are computed for each longitude point of the grid:

$$\mathrm{GHGS} = \frac{Z(\phi_o) - Z(\phi_s)}{(\phi_o - \phi_s)},$$

$$\mathrm{GHGN} = \frac{Z(\phi_n) - Z(\phi_o)}{(\phi_n - \phi_o)},$$

where

$\phi_n = 80°\mathrm{N} + \Delta$,
$\phi_o = 60°\mathrm{N} + \Delta$,
$\phi_s = 40°\mathrm{N} + \Delta$,
$\Delta = -4°, 0°$ or $4°$.

A given longitude is then defined as "blocked" at a specific instant in time if the following conditions are satisfied for at least one value of Δ:

(1) $\mathrm{GHGS} > 0$,

(2) $\mathrm{GHGN} < -10$ m/deg lat.

We decided to restrict Lejenäs and Økland's criterion (that is essentially equivalent to condition (1) alone) because we found that the addition of condition (2) was successfully eliminating from the "blocking catalogue" situations of large southward displacement of the midlatitude westerly jet that marginally satisfy condition (1) but not condition (2) and that, synoptically, would not be generally recognized as blocked.

3. The overall model performance in representing blocking

We start by showing the behaviour of the objective (local and instantaneous) index as a function of longitude. Fig. 1 shows the percentage frequency of blocking (objectively defined as above) as a function of longitude and computed on all ECMWF daily objective analyses of our database. Remembering that we have restricted our analysis to the winter period, this figure can be compared with Fig. 3 of Lejenäs and Økland (1983), showing that our modified version of their index behaves in a very similar way as far as the dependency on longitude is concerned. The two-well known maxima of frequency in the Euro-Atlantic and Pacific regions are well reproduced and a further secondary maximum around 50°E is also noticeable, associated with the relatively (and synoptically well known) frequent occurrence of Euro-Asian blocks. The two shaded regions also appearing in the figure will be used later in Section 4 to define objectively the concept of "blocked sector".

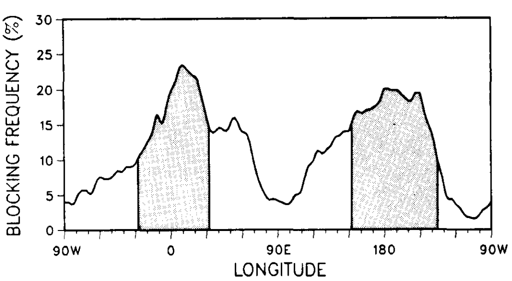

Fig. 1. Percentage frequency of blocking (objectively defined in Section 2) as a function of longitude and computed on all ECMWF daily objective analyses of our database.

Fig 2 shows again the same diagram of Fig. 1, but superimposed onto the corresponding diagram computed from the forecast fields, for days 1, 3, 6 and 10 (panels a to d respectively). This comparison allows us to document the progressive degradation of the performance of the operational forecasts for increasing forecast time. This degradation appears as a progressive loss of the amplitude of the two main blocking frequency maxima until, by day 10, the forecast maxima show approximately one half of the observed amplitude and also fairly appreciable phase shifts. More specifically, the Euro-Atlantic maximum has been shifted eastward by approximately 20°, while the Pacific maximum

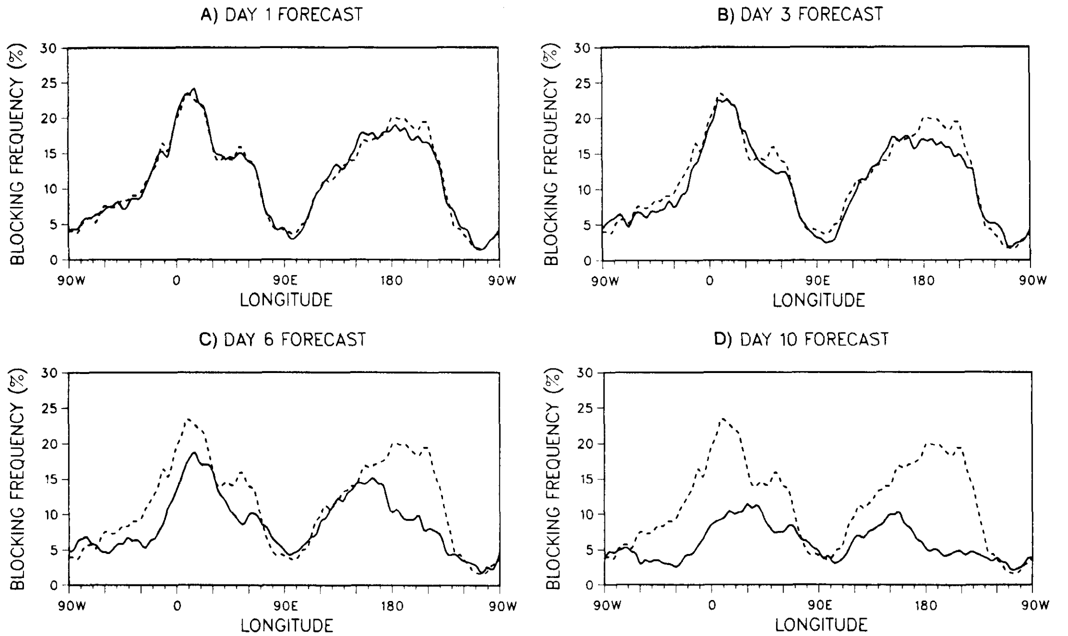

Fig. 2. Dashed lines: as in Fig. 1. Full lines: blocking frequency computed on the forecast fields, for days 1, 3, 6 and 10 (panels (a) to (d) respectively).

has been shifted westward by an even greater quantity, approximately 40° to 50°.

Such model behaviour is quite consistent with the well known deficiencies of general circulation models in general (and of the ECMWF GCM in particular). It has in fact been well documented (e.g., Hollingsworth et al., 1980; Bengtsson and Simmons, 1982; Wallace et al., 1983; Bettge, 1983; Arpe and Klinker, 1986; Palmer et al., 1986; Tibaldi et al., 1987) that GCMs tend to move, with increasing integration time, towards a climate "of their own" with increased mid latitude westerlies and decreased amplitude of planetary scale quasi-stationary waves. A variety of hypotheses have been put forward as to the possible causes for such behaviour (representation of mountains, horizontal and vertical diffusion, parameterization of convection etc., see many of the works quoted above), but the fact remains that such a model-produced climate is consistent with the apparent inability of the ECMWF GCM to reproduce the observed blocking frequency maxima at the proper longitudes. We will comment further in Section 6 of this fact when we will analyze the relationships between representation of blocking and model systematic errors.

We now want to investigate, within the limitations imposed by the dataset at our disposal, whether the main model changes that have taken place during the period considered here have had an impact on the ability of the operational forecasting system to represent blocking. Of course, this man-produced variability of the model performance overlaps and interacts with the natural year-to-year variability of blocking frequency and of circulation types. We have computed observed and forecast blocking frequency for three separate two-winter periods: 1981–82 and 82–83; 83–84 and 84–85; 85–86 and 86–87. In the first period, the operational model was an N48 grid-point model (48 grid intervals between poles and equator) with a grid-box-mean orography. In the second period the model was a T63 spectral model (triangular truncation at wavenumber 63) with a $\sqrt{2}\,\sigma$ envelope orography and in the third period a T106 spectral model with a 1 σ envelope orography. (If μ and σ are the mean and the standard deviation of the actual height of the surface within a grid-box of the model, an envelope orography is defined by setting the model surface height to $\mu + \alpha\sigma$, where $\alpha = \sqrt{2}$ in the T63 model, $\alpha = 1$ in the T106 model; see Wallace et al., 1983, and Tibaldi, 1986, for further explanation). We decided to exclude the first winter (1980–81) from this particular stratification of the analysis, because the model was at a preliminary stage of development and the model orography was excessively smooth; in addition, this orography was used during a one winter period only, while all the other three periods cover two winters. Figs. 3 to 5 show graphs similar to those in Fig. 2 but for the three two-winter periods separately (panels a to c) and for forecast days 3, 6 and 10 (Figs. 3, 4 and 5 respectively).

The first consideration we should make is that a large interannual variability is evident, with the second two-winter period showing an anomalously high frequency of those Euro-Asian blocked situations mentioned above. Their almost complete absence from the other two periods makes it obvious that the secondary maximum of frequency apparent in Fig. 1 around 50°E is almost completely due to episodes taking place during the winters of 1983–84 and/or 1984–85. Secondly,

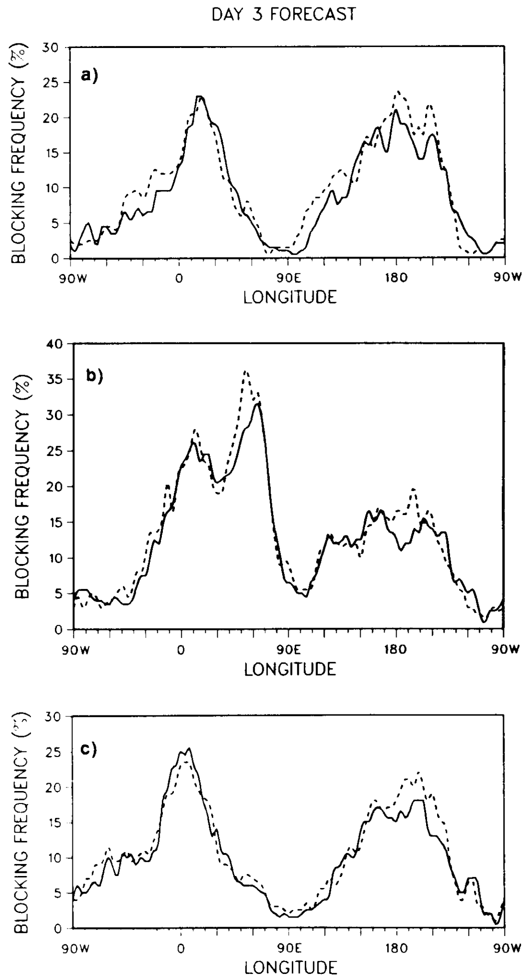

Fig. 3. As in Fig. 2, but for forecast day 3 only and for 3 two-winter periods separately: (a) 1981/82 and 1982/83; (b) 1983/84 and 1984/85; (c) 1985/86 and 1986/87.

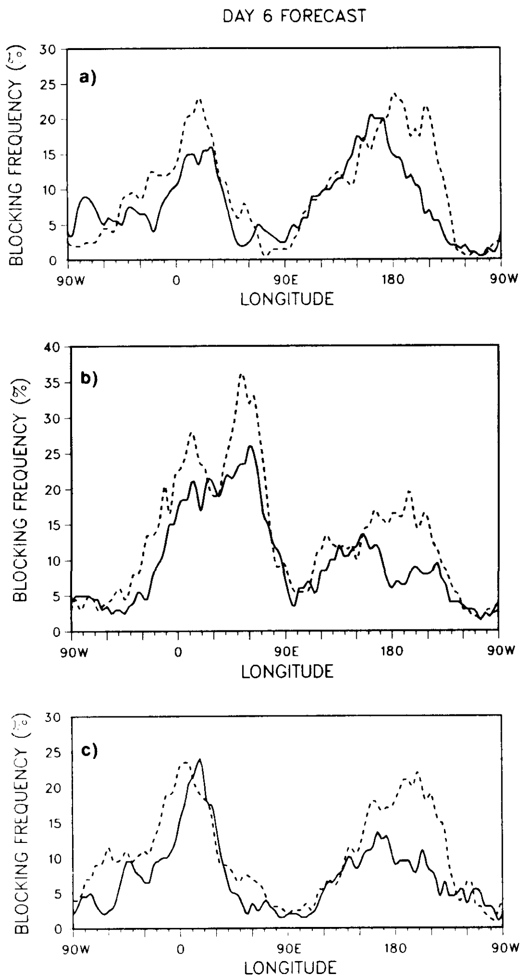

Fig. 4. As in Fig. 3, but for forecast day 6.

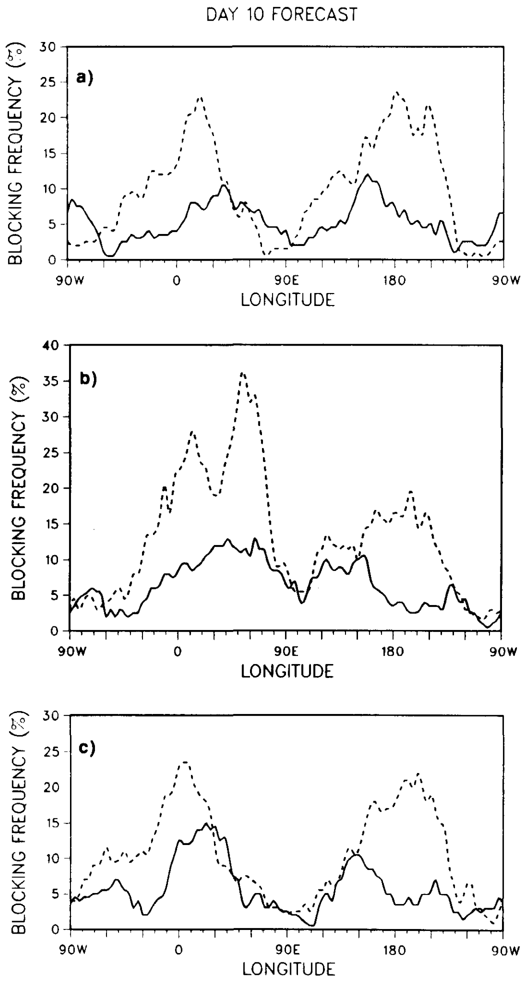

Fig. 5. As in Fig. 3, but for forecast day 10.

it is evident that the model's inability to represent blocking at an advanced stage during the forecast is not confined to any particular winter and has improved little with time and model development. The only notable exception to this is medium-range (day 6) Euro-Atlantic blocking during the 3rd 2-year period (Fig. 4c), apparently much better represented than in other periods for the same forecast time. Unfortunately, our sample is insufficient to substantiate this statistically, and in fact a similar (albeit less evident) behaviour can be seen in Fig. 4a for Pacific blocking. Since this panel refers to an old version of the model (that hopefully has been improved upon since then), we must conclude that both these episodes of variability in model performance might be due to poor sampling, rather than to systematic differences in model ability.

4. Euro-Atlantic and Pacific blocking

So far we have only very broadly examined the model's ability to represent local and instantaneous blocking conditions as defined by our objective index, as a function of longitude and forecast time. We want now to be able to distinguish between Euro-Atlantic and Pacific blocking in such an analysis. For this purpose, we need to develop further our objective definition of blocking so that it will allow us to define a blocked "sector". We do so by defining the two sectors (Euro-Atlantic and Pacific) as the two longitude bands that appear shaded in Fig. 1 (Euro-Atlantic from 28°W to 32°E and Pacific from 152°E to 224°E) and then by assuming that a sector is "blocked" if at least three adjacent grid points are blocked. This criterion requires, for a sector to be considered as blocked, that we have a region of zero or negative geostrophic westerlies extending for at least 12° longitude. With this criterion, on a total number of 700 days, we have 278 unblocked ("zonal") days, 422 blocked days (in either one or in both sectors), 273 Euro-Atlantic blocked days *and* 285 Pacific blocked days. $(273+285)-422=136$ is the number of days with both Euro-Atlantic and Pacific sectors blocked. Before turning our attention to the model performance, let us examine briefly some characteristics of the "observed" blocking.

Fig. 6 shows the distribution of the percentage of blocked days for the two sectors separately and for blocking in general (either one of the two sectors blocked) as a function of time (within the 100-day extended winter period we have considered). This is useful to highlight a possible seasonal trend, if there is one. Indeed the histograms show that the probability to have blocking (in either sector) increases considerably with time. Fig. 7, conversely, shows how blocking days are distributed as a function of the amplitude of the block itself, at least as this is represented by the amplitude of the GHGS gradient

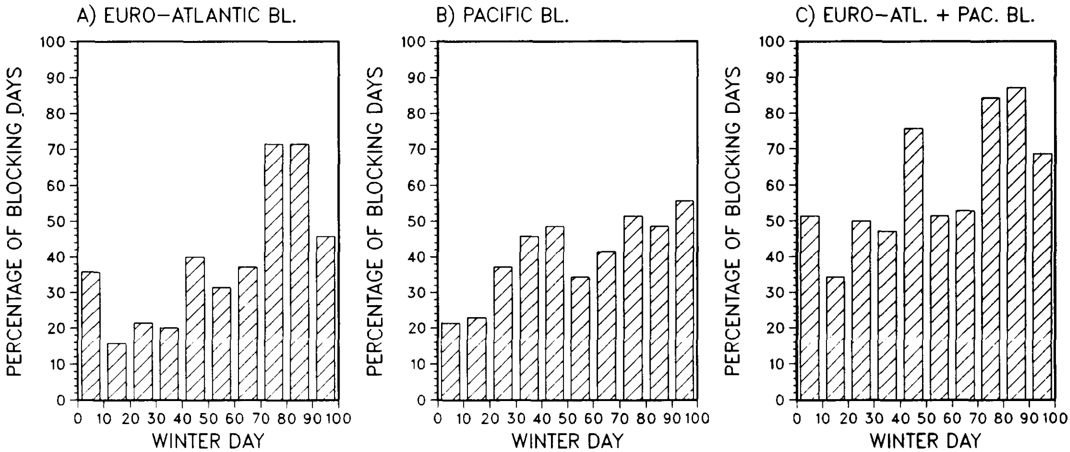

Fig. 6. Percentage of blocked days for the Euro-Atlantic sector (a), the Pacific sector (b) and for blocking in general (either one of the two sectors blocked) (c) as a function of seasonal time (within the 100-day winter period).

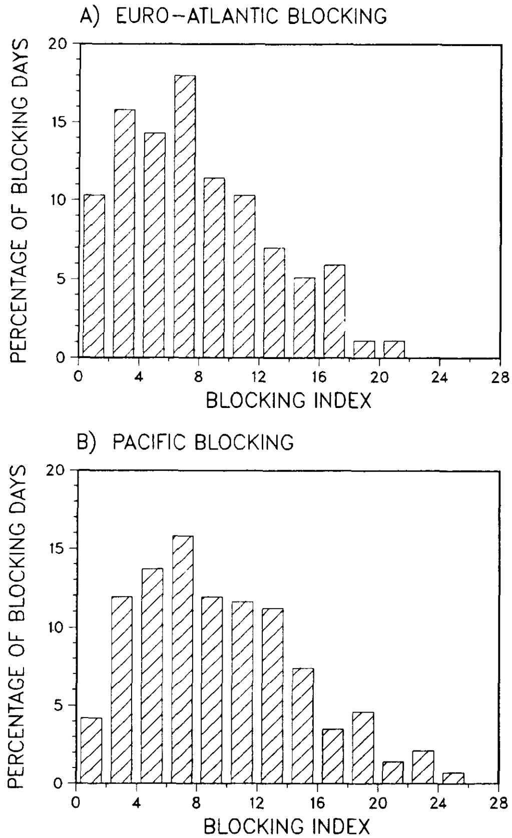

Fig. 7. Distribution of blocking days as a function of the amplitude of the block itself, as represented by the maximum value of the GHGS index (in m/deg); (a) Euro-Atlantic blocking; (b) Pacific blocking.

defined in Section 2 (essentially proportional to the strength of the geostrophic easterlies). Intense Pacific blocks appear to be relatively more probable that their Euro-Atlantic counterparts; the reverse is true for very weak blocks.

Turning now our attention to model performance, Fig. 8 shows the total number of blocked days in the forecast for the two separate sectors, as a function of forecast time. Forecast day 0 indicates the analyzed ("observed") values. The shaded portion of the histogram bars indicates the contribution to the total from those days that are correctly forecast as blocked, while the topmost blank part of the bars indicates the contribution from those days that are erroneously forecast as blocked, i.e., that are blocked in the forecast but not in the verifying analysis. The main indication of the results shown in Fig. 8 is that, by day 10, the forecasts for the Euro-Atlantic sector are blocked in a number of days that is only 50% of the observed total (see, for example, also Fig. 2d). However, half of the forecast blocked days are not verified by the corresponding analysis, leaving the total number of correct (verified) 10 day forecasts of blocking at only 25% of the observed. The situation for the Pacific sector is only marginally better, see Fig. 8b.

We are now interested in diagnosing whether the model, even in those cases for which it is correctly forecasting a blocked sector, does so with systematic amplitude and phase (longitude)

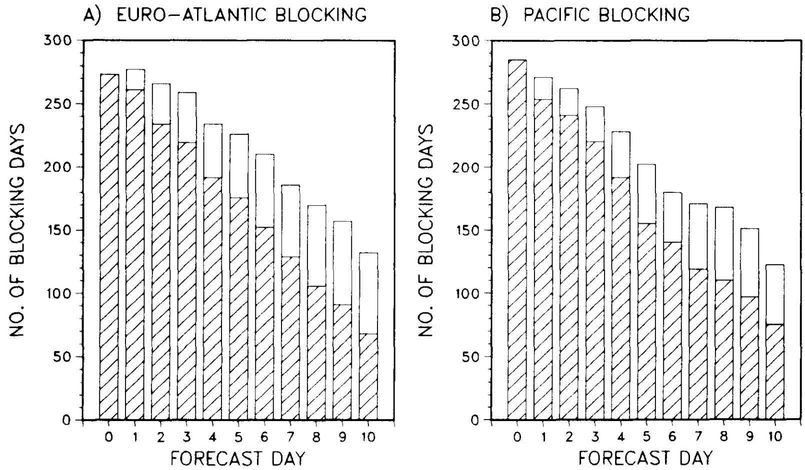

Fig. 8. Total number of blocked days in the forecast for the Euro-Atlantic (a) and the Pacific (b) sectors as a function of forecast time. Forecast day 0 indicates the analyzed values. The shaded portion of the bars indicates the number of days that are correctly forecast as blocked; the topmost blank part of the bars represents the days that are blocked in the forecast but not in the verifying analysis.

errors. Our index allows such an estimate if we interpret the maximum value of the GHGS index (in units of geopotential metres per degrees latitude) in the blocked sector as a measure of the amplitude of the block and the longitude of this maximum as a measure of the phase. Fig. 9 shows mean errors in the index value and in longitude (amplitude and phase errors) as a function of forecast time. Here we can confirm quantitatively what could already be qualitatively seen from Fig. 2: the model tends to shift Euro-Atlantic blocks progressively eastward, while it shifts the Pacific blocks westward (Fig. 9b). The model also loses amplitude in both sectors; but the amplitude loss seems to take place more rapidly in the case of Pacific blocks. (The apparent recovery in the mean errors that can be seen after day 7, especially in the case of Pacific blocking, is possibly due to the fact that only very persistent blocks are still detectable in the forecast after one week, so that the statistics displayed in Fig. 9 become representative only of the most predictable cases.) Such differences of modelling characteristics suggest that the contribution given by various physical mechanisms to the maintenance of blocks might be (at least partially) different in the two sectors.

5. Modelling blocking onset and maintenance

It is conceivable (and many theoreticians and synopticians have speculated along this line of thought) that different physical mechanisms are to be held responsible for blocking onset and for blocking maintenance. If blocking is indeed a metastable "state" (global or local is of little consequence, at this stage of the argument) which the atmosphere enters as a result of an instability mechanism (e.g., Charney and DeVore, 1979; Charney and Strauss, 1980; Källén, 1982; Malguzzi and Speranza, 1981; Speranza, 1986; Benzi et al., 1986a; Benzi et al., 1986b) then it should be a priori expected that during highly unstable situations (as immediately before and during the onset) numerical forecasting should be a daunting task; on the contrary in fairly stable conditions (as when a block is well established) forecasting should be a more tractable problem. It is, in fact, a widespread belief that numerical models have, in general, more difficulties in entering a blocked situation than they have in maintaining a block once this is already present in the initial conditions from which the integration is started. We want now to address this problem by analysing separately blocking onset

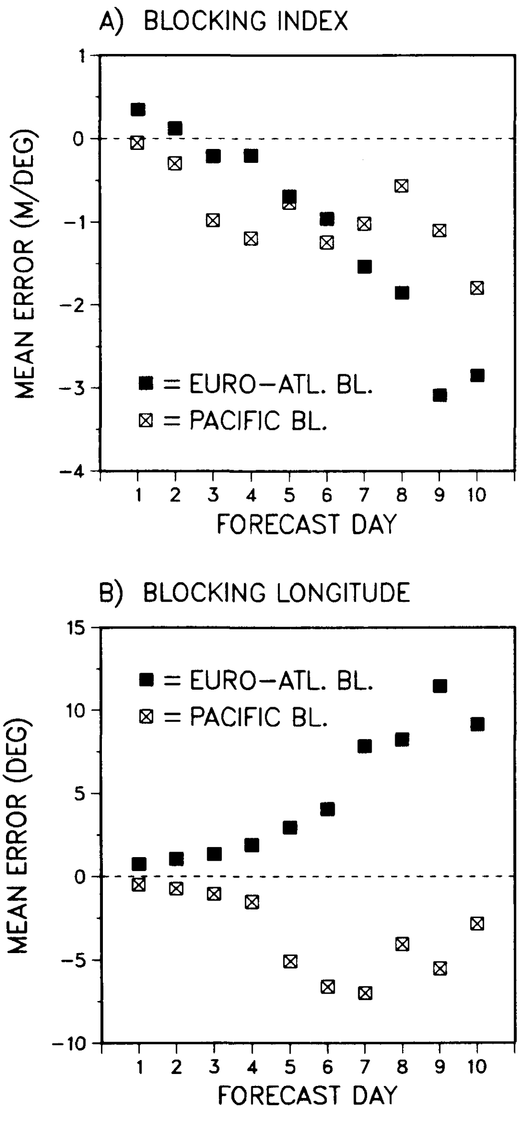

Fig. 9. Mean errors in the maximum value of the GHGS index (a) and in the corresponding longitude (b) (blocking amplitude and phase errors) as a function of forecast time.

and blocking maintenance and the model's ability at reproducing both. To do this we need once more to restrict our definition of blocking in order to be able to define "episodes" objectively; in a very simple and straightforward manner we decided to define a "blocking episode" as a period during which a sector is blocked for at least four consecutive days according to the observed data. With this definition, we found 22 cases of Euro-Atlantic and 24 cases of Pacific blocking in our 700 days dataset. We shall now concentrate on blocking onset first.

Fig. 10 attempts to show the model's ability to forecast blocking onset. Each of the 22 Euro-Atlantic (panel a) and 24 Pacific (panel b) cases is represented by one column. A black square at forecast day n indicates that the forecast verifying on the first day of the blocked period (the blocking "onset") and started n days before was also blocked according to our criterion; a hollow square indicates a failure. Obviously, all squares are black at forecast day 0 (the analysis) and most of them are black at forecast day 1, indicating that very short-range forecast of blocking onset is fairly successful (not completely, however; on a total of $22 + 24 = 46$ cases, 8 failed, although in 4 such failures some previous longer-range forecasts had given the correct indication). The general picture is one of some almost complete failures, some (less, however) outstanding successes and many ordinary cases in which the forecast gives good guidance up to 3 to 4 days in advance. There seems to be, this time, no obvious and systematic difference of model behaviour between the two sectors, but also no obvious trend in model performance from winter to winter (the cases belonging to different years are grouped together and time increases from left to right). The overall results are somewhat disappointing, but we would like to remind the reader that it is highly likely that a good synoptician can extract useful guidance from the forecast maps even for some of those cases that have been penalized by the objective indicator. In fact, if our criterion is only marginally satisfied by the analysis, even a small difference in the circulation pattern can affect the classification of the forecast. To test the sensitivity of our objective definition of onset, we have computed the same diagrams as in Fig. 10, but for the second day of each blocking episode (Fig. 11). Indeed, the performance of the forecasting model appears to be better in this case, which is partially due to the stronger blocking signature but also to the fact that the initial conditions are one day closer to the actual onset for a given forecast time.

To summarize the results on the diagnostics of forecast of blocking onset we present four

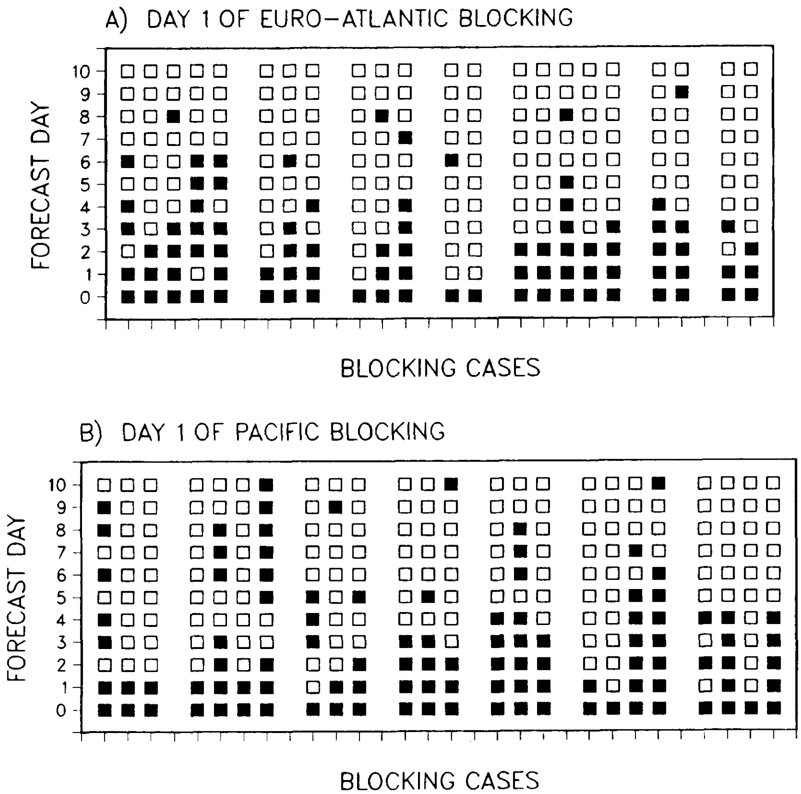

Fig. 10. Diagram of successful (black squares) and unsuccessful (hollow squares) forecasts of the observed blocked regime in the first day of each of 22 Euro-Atlantic (a) and 24 Pacific (b) blocking episodes, as a function of the forecast time. Cases belonging to the same winter are grouped together.

histograms in Fig. 12. Each panel gives the number of cases of blocking onset correctly forecast as a function of forecast lead time. For the first day of blocking, the model data appear to contain little useful information on the onset beyond forecast day 3, with very little difference between the two sectors. The impression received by comparing qualitatively Figs. 10 and 11 is here confirmed more quantitatively: forecasting the *second* day of blocking is measurably more successful than forecasting the first day: at forecast day 3 we have 11 successful predictions of the first day in the Euro-Atlantic sector against 16 good forecasts of the second day (on a total of 22 cases). The respective figures for the Pacific sector are 12 against 21 over a total of 24. In most cases, the day n + 1 forecast of the second day of blocking is better than the day n forecast of the first day (these two forecasts come from the same model integration, started from the initial conditions analyzed n days before the onset of the block). For example, we have 13 and 15 good 4-day forecasts of the second day of the block against 11 and 12 3-day forecasts of the first day (Euro-Atlantic and Pacific sectors respectively). This would suggest that transitions to blocking occur more slowly in the model than in the actual atmosphere.

We now move to blocking maintenance (or, more precisely, duration). We will restrict our analysis to those forecasts that start from the first day of a blocking episode; therefore, from an initial condition that already contains a block in at least one of the two sectors under analysis. Fig. 13 has the same general layout of Fig. 11, but now the vertical bars indicate both analyzed and

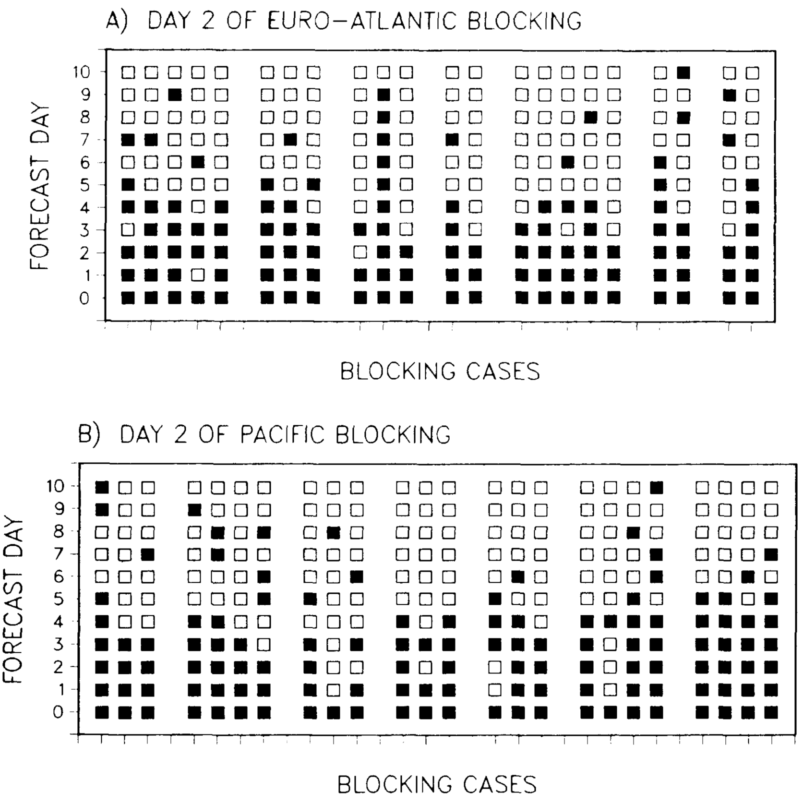

Fig. 11. As in Fig. 10, but for the second day of each blocking episode.

forecast duration (white and shaded bars, respectively). The cases are, of course, the same as for Fig. 11. So, if the topmost portion of the vertical bar is shaded, the forecast duration is longer than the observed. If the topmost part of the bar is white, the reverse is true. In case of a "perfect" forecast, the bar is completely shaded. A duration (either observed or forecast) of 11 days signifies a duration longer than 10 days.

Even though predicted blocks either shorter or longer than observed are quite common, the overall performance of the model appears to be more satisfactory than in the case of blocking onset; a few outstanding successes in forecasting blocking duration longer than 10 days are apparent in both sectors. A closer look at the precise figures reveals that, on average, the model is in fact underestimating blocking duration; this is shown more clearly in Fig. 14, where histograms of the number of cases as a function of duration are displayed for the two sectors separately, as usual. While no observed case shorter than four days is present (by definition of episode), respectively 5 and 4 cases of shorter blocks occur in the two sectors in the forecast. Conversely, the number of analyzed blocks longer than 10 days is always higher than the corresponding forecast number (only 6 against 5 for the Euro-Atlantic sector, but 10 against 4, a much larger error, for the Pacific sector).

The different skill of the model in forecasting the duration of long-lived blocks over the Euro-Atlantic and the Pacific sector again suggests the possibility of differences in the contribution of various physical processes to the maintenance of blocking in the two sectors. For example, the relevance of the transient eddy forcing mechanism proposed by Green (1977) has been clearly documented in a number of papers for the Atlantic blocking (see for example Illari and Marshall,

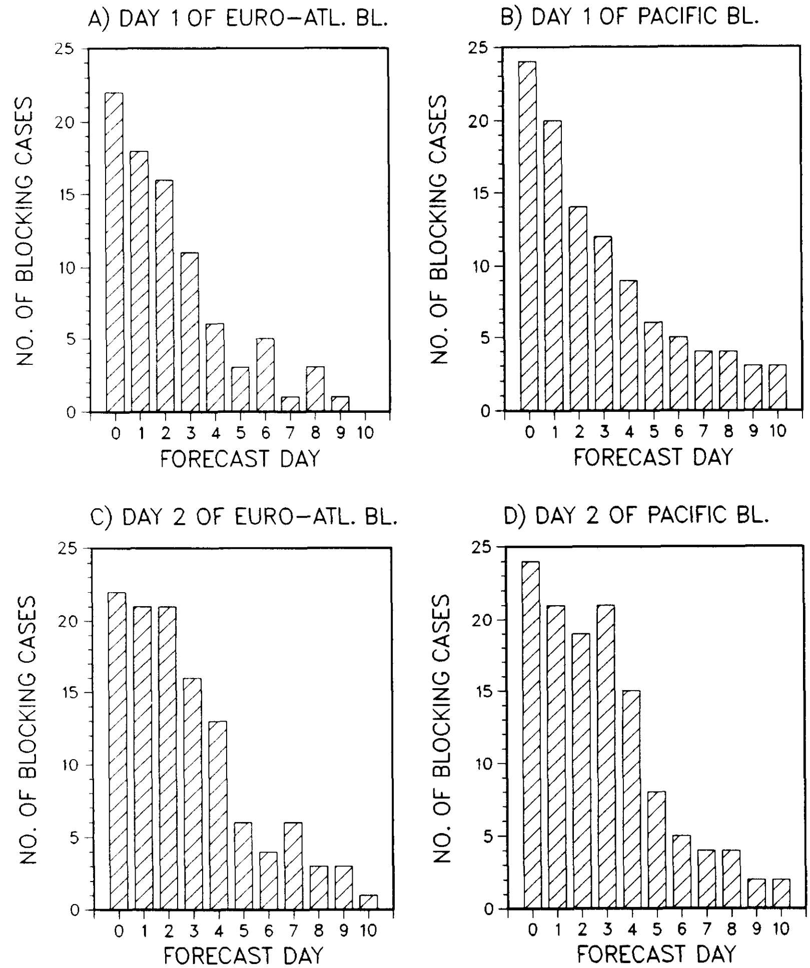

Fig. 12. Number of cases of blocking onset correctly forecast as a function of forecast lead time. Panels (a) and (b) refer to the first day of the blocking episodes, panels (c) and (d) to the second day. Panels (a) and (c) refer to Euro-Atlantic blocking, panels (b) and (d) to Pacific blocking.

1983; Shutts, 1986; Hoskins and Sardeshmukh, 1987), but comparable evidence has not yet been provided for Pacific cases.

The results discussed above indicate that the ECMWF model performed better when a block was already in the initial conditions than in cases of transitions from a zonal to a blocking state. However, the use of our simple blocking indicator does not allow a precise quantitative comparison between the model performances in the two cases. For this purpose, we can turn to a more traditional skill score, the anomaly correlation coefficient (ACC) between observed and predicted fields (again of 500 hPa height) over the two sectors used for the definition of blocking episodes (the latitudinal limits of the sectors have been set to 84°N and 36°N).

For each of the Euro-Atlantic and the Pacific blocking episodes, we have computed ACC's from forecast days 1 to 10 for: (a) the 3 forecasts that started on the day of the blocking onset, 1 and 2 days later; (b) the 3 forecasts that started 4, 5 and 6 days before the day of the blocking onset. In addition, we have computed ACC's for: (c) all

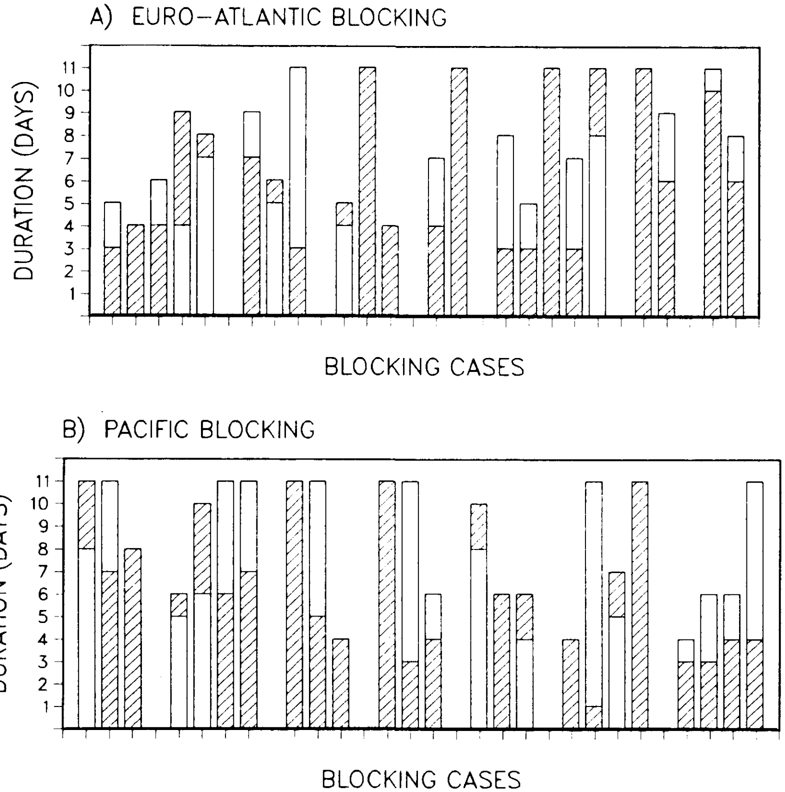

Fig. 13. Duration of the 22 Euro-Atlantic (a) and 24 Pacific (b) blocking episodes as deduced from the analysis (white bars) and from the forecast started on the first day of each episode (shaded bars). A duration of 11 days indicates any duration longer than 10 days. The white bar is fully covered by the shaded bar when the forecast duration equals the observed one.

the forecasts that had no blocking at all throughout the integration period.

The scores for all the forecasts in groups (a), (b) and (c) have been averaged, and are displayed in Fig. 15 for the two sectors separately; the three groups are labelled as "blocking", "transition" and "zonal" respectively. A weighted average has been used for the "zonal" group, in order to have a contribution from each winter proportional to the number of blocking cases in the winter; in this way, changes in the forecast model affect all the three groups in the same way.

In both sectors, the "transition" forecasts have clearly the worst ACC's, much lower than the scores of the "blocking" forecasts. A difference between the two sectors can be seen with regard to the skill of the "zonal" forecasts; they are marginally more skilful than the "blocking" forecasts in the Euro-Atlantic sector, worse (and closer to the "transition" forecasts) in the Pacific sector. On the other hand, when the actual values of ACC in the two sectors are compared, one can see that in the last 5 days, the scores for the "zonal" forecasts are generally closer than those for the "blocking" and "transition" forecast: ACC's for these two groups are higher in the Pacific than in the Euro-Atlantic sector.

This particular result does not appear to be in complete agreement with our previous statistics about blocking maintenance based on the blocking indicator. However, one must realize that the ACC over a sector covering about 60° of longitude is sensitive not only to the block itself but also to the large-scale flow in which the block

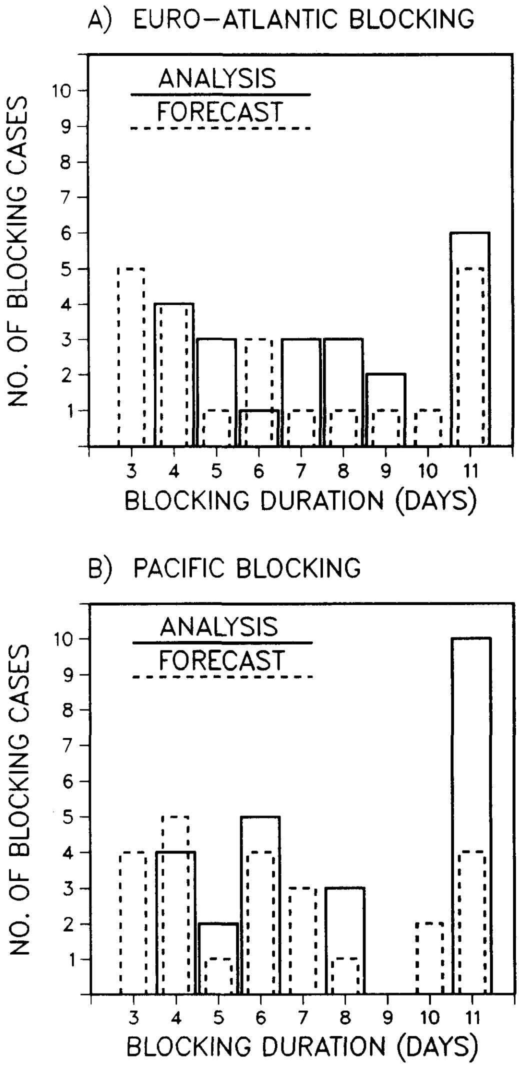

Fig. 14. Histograms of the number of blocking cases as a function of duration for the Euro-Atlantic (a) and the Pacific (b) sector.

is embedded. In the Pacific area, blocks often occur within a large area of positive geopotential anomaly, which covers most of the central and eastern Pacific at high latitudes and can be seen as a part of the standing oscillation pattern known as the Pacific-North American (PNA) pattern (Wallace and Gutzler, 1981). Even if the forecast fails to reproduce the dipole structure of the block and reduces the amplitude of the PNA

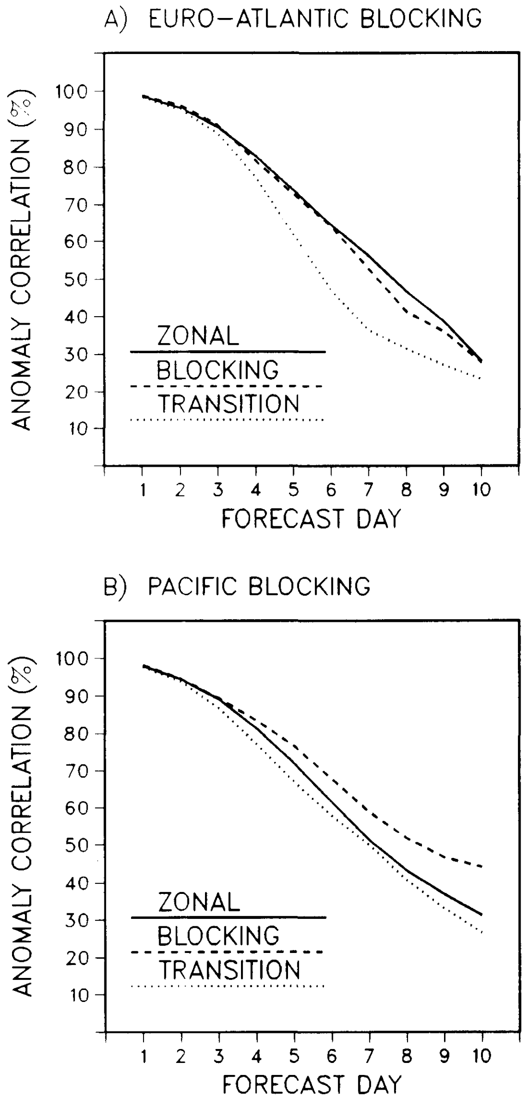

Fig. 15. Average curves of anomaly correlation coefficients over the Euro-Atlantic (top panel) and the Pacific sector (bottom panel) for forecasts started on the day of a blocking onset, 1 or 2 days later (blocking); for forecasts started 4, 5 or 6 days before the onset (transition); and for forecasts with no blocking during the integration period (zonal).

pattern, but predicts its phase in the correct way, this is likely to give a relatively high value of ACC. Over the Euro-Atlantic sector, there is no single, dominant steady oscillation pattern like the PNA. Blocks often occur in the ridging part of a wave pattern, the phase of which is not as fixed as in the PNA case (the European mountain chains are much less effective than the Rockies in locking the phase of the large-scale waves). In this situation, a shift in the predicted wave pattern can negatively affect the anomaly correlation, even if a block is still present in the forecast (see the larger errors in blocking longitude for the Euro-Atlantic area than for the Pacific area, shown in Fig. 9b).

Apart from these considerations, what we want to stress here is the sharp difference in predictability between the cases in which a transition to blocking occurs in the middle of a 10-day forecast and those in which a block is already present in the initial conditions. If we measure the usefulness of a forecast by the duration of the period in which the ACC remains above 0.6 (a practical rule often used at ECMWF), the difference in predictability between the "blocking" and the "transition" forecasts is 1.2 days in the Euro-Atlantic sector, 1.1 days in the Pacific sector. These differences are comparable with the average gain due to the improvements in the ECMWF model over many years of operational activity.

6. Model systematic errors and blocking

The problem of climate drift in General Circulation Models has long been recognized as one of major concern and has received much attention in recent years (for a few examples, see the works quoted at the beginning of Section 3). Our perception of model systematic error as revealed by a large (but seasonally homogeneous) ensemble mean of forecast error fields would have to be taken with caution if it could be shown with certainty that the distribution in phase space of possible atmospheric states is not unimodal.

Let us consider, for example, the case of an atmosphere with two distinct regimes, corresponding to different quasi-stationary states, and let us assume that the two regimes have a different amplitude of the planetary waves. Let us also consider two different models of such an atmosphere, both of them possessing two regimes: in the first one, the two regimes occur with the same frequency as in the real atmosphere, but each of the two regimes has a lower wave amplitude than the corresponding atmospheric state; in the second one, the wave amplitude of the two regimes is correct, but the model enters the low-amplitude regime much more frequently than the real atmosphere. The "climate" of both these models will show a lower amplitude of the planetary waves when compared to the real atmosphere, but only in the first case the error can be really considered as "systematic".

Since convincing evidence of a multimodal distribution of atmospheric states is accumulating (Sutera, 1986; Hansen, 1986; Hansen and Sutera, 1986; Benzi et al., 1986a; Molteni et al., 1988) and since such atmospheric "modes" (or "states" or "regimes") have been often associated to the blocking phenomenon, it is of particular interest to diagnose model systematic errors using blocked and non-blocked ensembles separately.

We shall concentrate our analysis on the 10-day forecasts, and first of all we want to see if the differences in the circulation pattern between blocked and non-blocked situations are, on average, correctly forecast by the ECMWF model. For this purpose, we have computed mean fields of observed and forecast 500 hPa height for different groups of days, classified according to the occurrence of blocking *in the verifying analysis:* the 422 days on which a block occurred in either the Euro-Atlantic or the Pacific sector; the 273 days on which a Euro-Atlantic block occurred; the 285 days on which a Pacific block occurred; the 278 "zonal" days, that is, the days when no block occurred.

Subsequently, for both the analysis and the forecast, we have computed the differences between the first three mean fields and the fourth. These difference maps are shown in Fig. 16 (analysis) and Fig. 17 (10-day forecast); in the figures, both the full fields and their eddy component (that is, their deviations from zonal means) are displayed.

When considering the observed fields (Fig. 16), the blocking dipolar structures are quite evident in the respective quadrants. What was perhaps less obvious to expect is the signal appearing over the North American continent in both panels (e) and (f), another dipole structure of the opposite sign of the blocking dipole (negative to the north and positive to the south). Obviously, the definition of eddy field itself requires a compen-

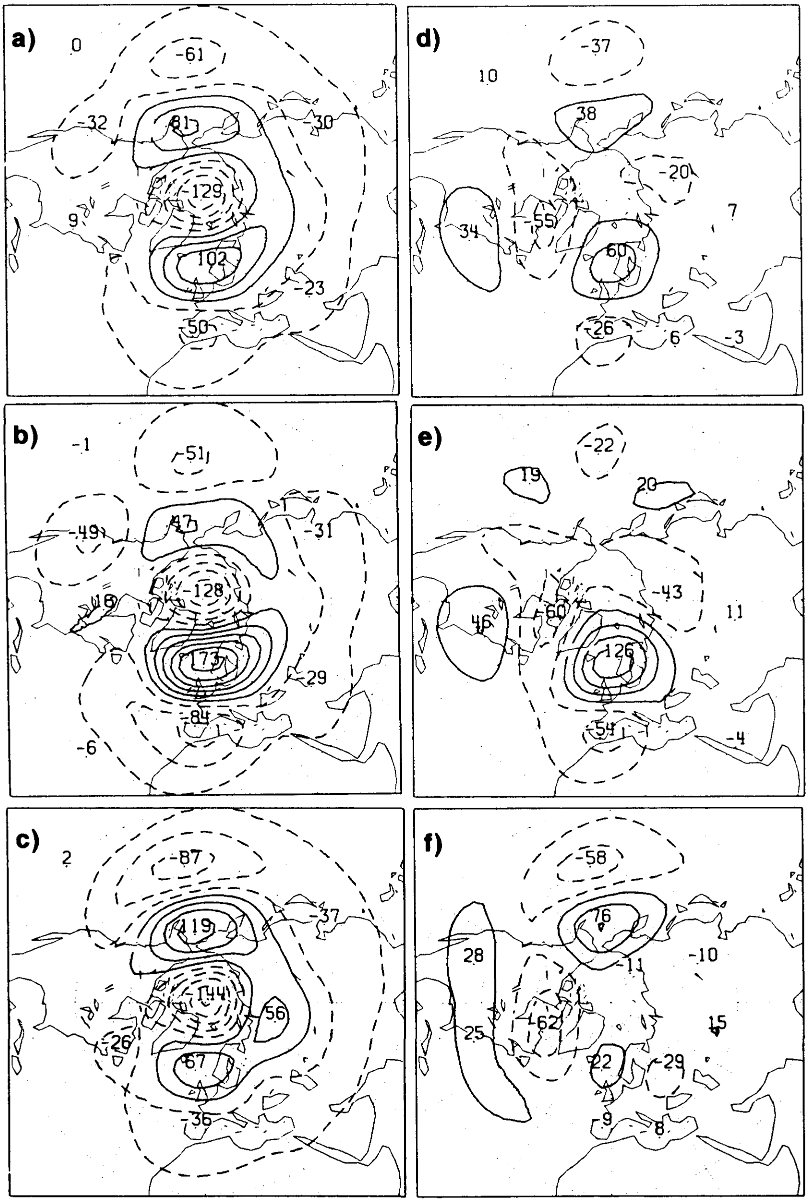

Fig. 16. (a) Difference between mean observed fields of 500 hPa height in the ensembles of "blocked" and "zonal" days (Blocking can be either in the Euro-Atlantic or in the Pacific sector). (b) as (a), but for Euro-Atlantic blocking only. (c) as (a), but for Pacific blocking only. (d), (e) and (f) as (a), (b), (c) respectively, but showing the eddy component of the difference fields.

sation of the blocking dipoles in order to obtain a zero-valued zonal mean. However, a priori there is no reason why these compensating features should be concentrated in a single region. In particular, one can note how a similar signal is completely absent from the Asian region.

When we turn to the forecast fields at day 10 (Fig. 17), the almost complete absence of signifi-

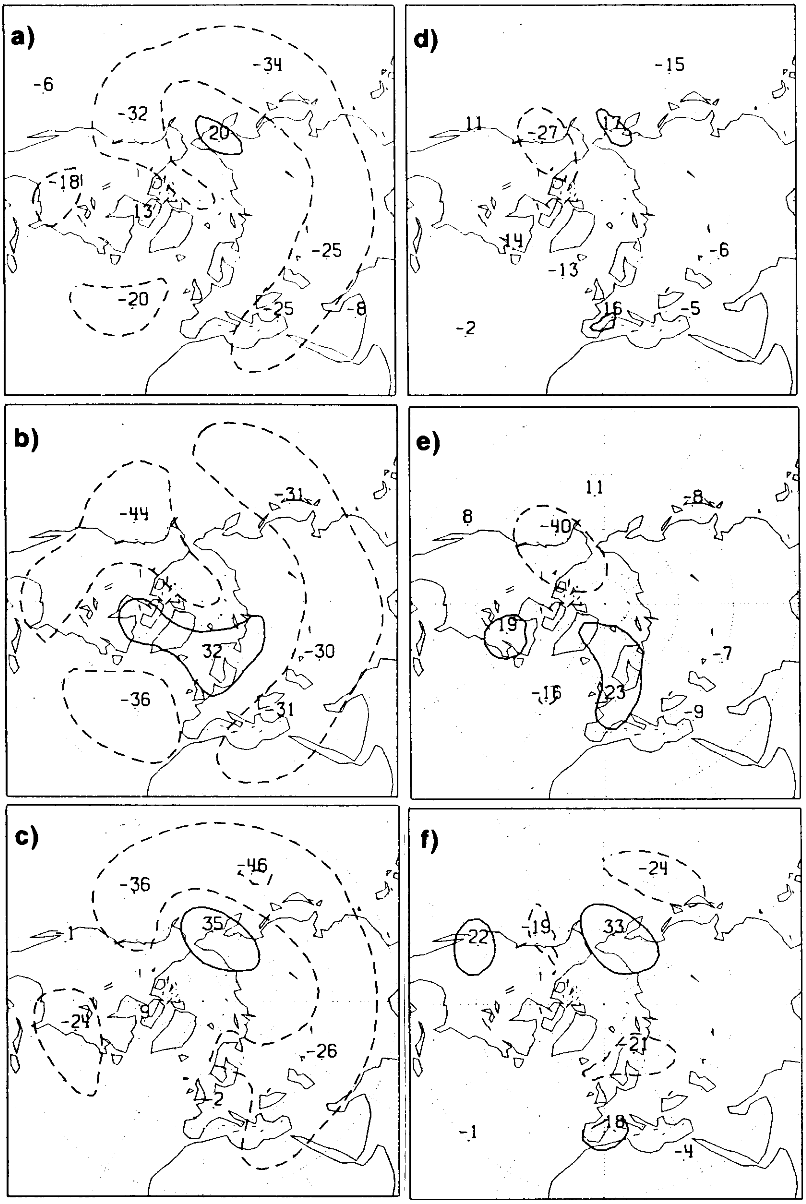

Fig. 17. As in Fig. 16 but deduced from means of 10-day forecast fields verifying on the same "zonal" or "blocked" days.

cant structures is striking and even more so for the eddy part of the fields (panels d to f). Essentially, the inability of the model in representing the observed blocks is reflected by the absence, in the ensemble mean maps, of those structures that are the essential signature of the actual atmospheric process.

Strictly speaking, what the lack of significant features in Fig. 17 implies is that, after 10 days, the model has lost the ability to distinguish

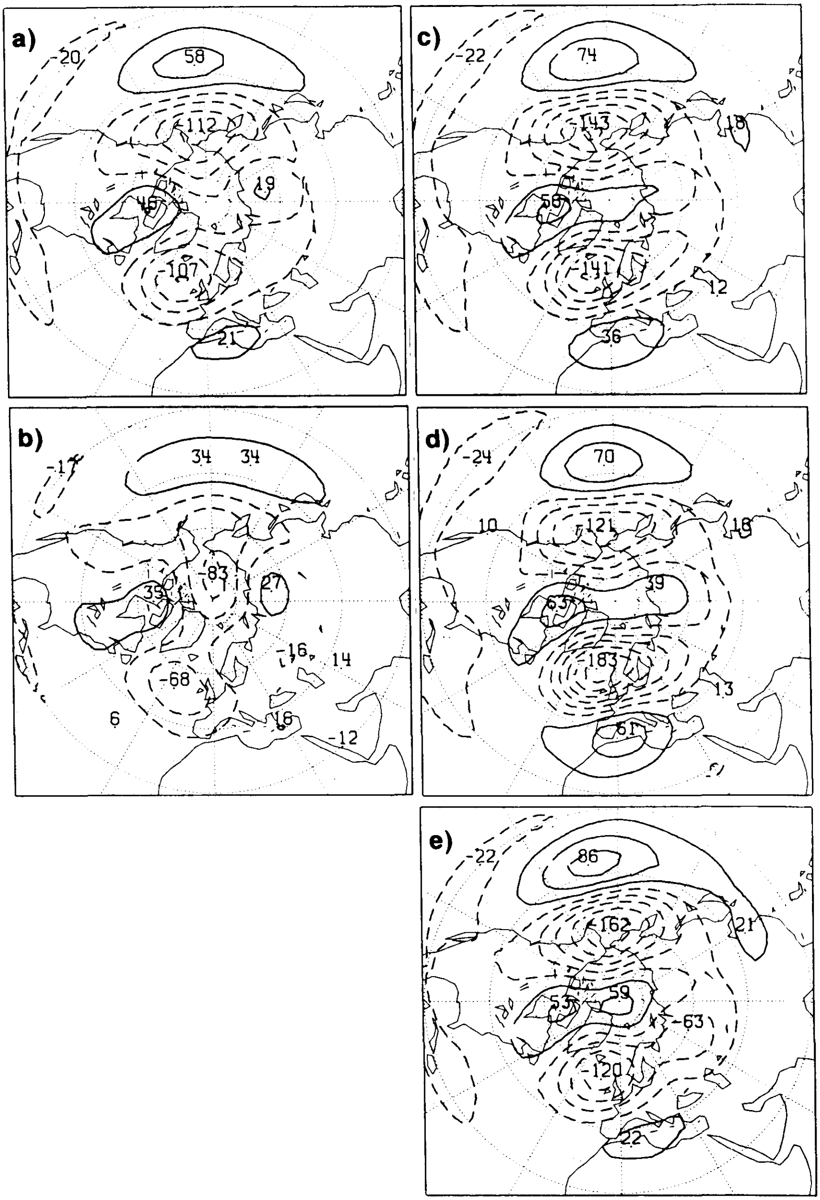

Fig. 18. Mean maps of 500 hPa height error at forecast day 10, computed from (a) the complete 700-day sample; (b) the 278 non-blocked, or "zonal" days; (c) the 422 blocked days; (d) the 273 Euro-Atlantic blocked days; (e) the 285 Pacific blocked days.

between a zonal and a blocked situation. No information about systematic errors can be deduced from this figure only. However, we have already shown in Section 3 that there is a considerably lower occurrence of blocking in the 10-day forecast. This suggests that the correct interpretation of Fig. 17 is that the mean state of the model in the actual blocking days is very similar to the observed mean zonal state.

This interpretation finds a clear confirmation

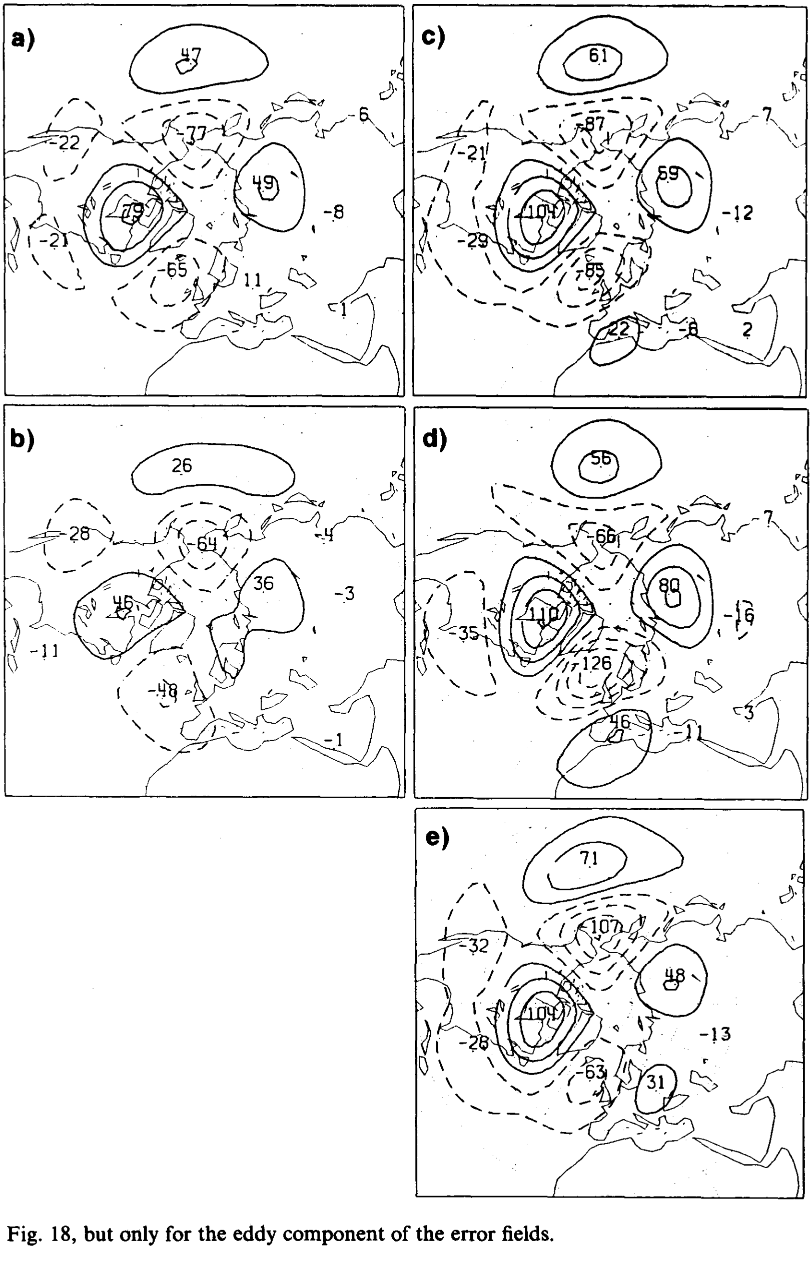

Fig. 19. As in Fig. 18, but only for the eddy component of the error fields.

when one looks at the mean error maps (i.e. forecast minus analysis) at day 10, computed from different sets of days, namely: (a) all the 700 days in our data set; (b) the 278 zonal days; (c) the 422 blocked days; (d) the 273 days with Euro-Atlantic blocking; (e) the 285 days with Pacific blocking.

These error maps are displayed in panels (a) to (e) of Fig. 18 as full fields, while their deviations from zonal means, which show the mean errors in the eddy fields, are presented in the corresponding panels of Fig. 19.

A direct comparison respectively between Figs. 16a, b, c and Figs. 18c, d, e (full fields) and

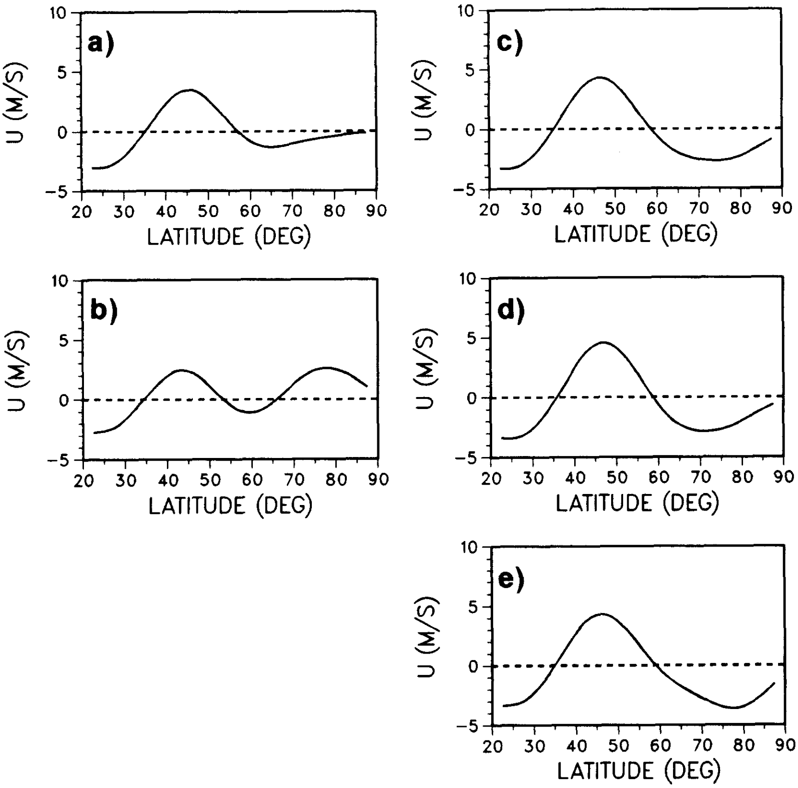

Fig. 20. Ensemble mean error of the zonally averaged geostrophic wind (in m/s) as a function of latitude for the same data stratification as in Fig. 18, panels (a) to (e).

between Figs. 16d, e, f and Figs. 19c, d, e (eddy component) confirms that the systematic error signatures are almost equal and opposite in sign to those characteristic of blocking. A further comparison of Fig. 19b with Figs. 19c, d, e reveals that, although the systematic error signature during non-blocked ("zonal") days is qualitatively not dissimilar to that characteristic of either Euro-Atlantic or Pacific blocking (essentially a structure dominated by zonal wavenumber two), its amplitude is quite different, and in fact much smaller. This is nothing but a quantitatively more accurate restatement of the fact that the model, well into the medium range (day 10), is unable to enter and/or to maintain blocking at the observed levels.

Fig. 20 shows the systematic error of the purely zonal part of the field (expressed in m/s of geostrophic wind as a function of latitude) during the different regimes. Even in this case, the systematic error during the blocked and non-blocked regimes is quite different (and the first dominates over the second in the total ensemble, see panel (a)). During zonal periods, the zonal systematic error (panel (b)) has the structure of a weak double band of excessive westerlies, around 45°N and 80°N, with an even weaker easterly band in between. At low latitudes, the error is easterly again. This error structure implies a northward shift of both the subtropical and the polar branches of the jet. During blocking (either Euro-Atlantic or Pacific), the structure of the systematic error is the familiar one, so often and exhaustively documented in the literature (see again the works mentioned above, in Section 3), that is one of a strong northward displacement of the subtropical jet and of strong reduction of the westerlies at high latitudes. In other words, the model tends to cancel the split of the jet that occurs in the actual atmosphere.

We can conclude that the fact that blocking is associated with an enhancement of the amplitude of the quasi-stationary planetary scale waves (e.g., Austin, 1980; Hansen and Chen, 1982; Ji and Tibaldi, 1983; Lejenäs and Döös, 1987), the fact that the model is often unable to predict an increase in the amplitude of the planetary waves beyond 3 to 4 days and the fact that the model is also not capable of entering blocking beyond 3 to 4 days into the forecast are connected facts. At this stage, it is impossible to ascertain whether the third is a cause or a consequence of the second. We have, however, shown that the well known zonal and eddy signature of the model systematic error is mostly produced during blocked situation; it therefore reflects the inability of the model to exit the zonal state and to enter the blocked state. What is the ultimate (or at least, the principal) cause of this inability is still an open question.

7. Summary and conclusions

We have used 7 100-day winter periods (1980–81 to 1986–87) of ECMWF operational 500 hPa height analyses and forecasts (days 1 to 10) to assess the skill of the Centre's model in short and medium range forecast of blocking. Firstly we have given an objective definition of blocking (following essentially Lejenäs and Økland, 1983) and we have diagnosed the behaviour of the model as a function of longitude and forecast day. We have also stratified the diagnosis for different 2-year periods during each of which the model characteristics remained almost unchanged. We then proceeded to distinguish between Euro-Atlantic and Pacific blocking by specifying an objective definition of "blocked sectors". In order to be able to analyze separately blocking onset and blocking maintenance, we further restricted our choice to episodes longer than three days (we found in this way 22 cases of Euro-Atlantic and 24 cases of Pacific blocking). We finally examined zonal and eddy components of model systematic errors during the so-defined circulation regimes.

On the basis of this diagnostic analysis we reached the following conclusions.

(a) Serious systematic deficiencies were found in the model simulation of blocking after forecast day 3 to 4: only about 50% of blocking days are found at forecast day 10 compared to the analysis, and approximately half of those do not correspond to actually observed blocked days.

(b) Only slight improvements were found in the model ability of reproducing blocking during the seven winters of operations analyzed.

(c) Differences between Euro-Atlantic and Pacific blocking forecasts were found with regard to increase in forecast quality during the years (as model resolution and physics improved), phase and amplitude errors, and skill in predicting the duration of blocks. Such differences might reflect different dominating mechanisms for the onset and maintenance of long-lived blocking structures in the two different sectors.

(d) Blocking onset is almost consistently missed by the model beyond forecast day 3 to 4; conversely, once blocking appears in the initial conditions, duration is reasonably well predicted into the medium range (although with some undererstimation).

(e) Systematic model errors appear to be strongly related to the inability of the model to represent the transition between "zonal" and blocked regimes. It would seem more appropriate to talk about a "systematic model regime" (the zonal one) rather than of a systematic model error. In fact, the zonal regime occurs in the model atmosphere with a much greater frequency than in the real atmosphere, and the cases in which the former is in the zonal state but the latter is in the blocked state account for a large proportion of the mean error of the model. It is our opinion that further investigations on the physical mechanisms that cause the onset of blocking will be able to throw more light onto possible causes of systematic errors in general circulation models.

REFERENCES

Arpe, K. and Klinker, E. 1986. Systematic errors of the ECMWF operational forecasting model in mid-latitudes. *Q. J. R. Meteorol. Soc. 112*, 181–202.

Austin, J. F. 1980. The blocking of middle latitude westerly winds by planetary waves. *Q. J. R. Meteorol. Soc. 106*, 327–350.

Bengtsson, L. 1981. Numerical prediction of atmospheric blocking. A case study. *Tellus 33*, 19–42.

Bengtsson, L. and Simmons, A. J. 1982. Medium range weather prediction—operational experience at ECMWF. In: *Large-scale dynamical processes in the atmosphere* (eds. B. J. Hoskins and R. P. Pearce.) New York: Academic Press, 337–363.

Benzi, R., Speranza, A. and Sutera, A. 1986a. A minimal baroclinic model for the statistical properties of low-frequency variability. *J. Atmos. Sci. 43*, 2962–2967.

Benzi, R., Malguzzi, P., Speranza, A. and Sutera, A. 1986b. The statistical properties of general atmospheric circulation: observational evidence and a minimal theory of bimodality. *Q.J.R. Meteorol. Soc. 112*, 661–674.

Benzi, R., Saltzman, B. and Wiin-Nielsen, A. C. (eds.), 1986c. Anomalous Atmospheric Flows and Blocking. *Advances in Geophysics 29*. New York: Academic Press.

Bettge, T. W. 1983. A systematic error comparison between the ECMWF and NMC prediction models. *Mon. Wea. Rev. 111*, 2385–2389.

Charney, J. G. and DeVore, J. G. 1979. Multiple flow equilibria and blocking. *J. Atmos. Sci. 36*, 1205–1216.

Charney, J. G. and Strauss, D. M. 1980. Form-drag instability, multiple equilibria and propagating planetary waves in baroclinic, orographically forced, planetary wave systems. *J. Atmos. Sci. 37*, 1157–1175.

Dole, R. M. and Gordon, N. D. 1983. Persistent anomalies of the extratropical northern hemisphere wintertime circulation: geographical distribution and regional persistence characteristics. *Mon. Wea. Rev. 111*, 1567–1586.

Green, J. S. A. 1977. The weather during July 1976: some dynamical considerations of the drought. *Weather 32*, 120–128.

Grønaas, S. 1982. Systematic error and forecast quality of ECMWF forecasts in different large-scale flow patterns. *ECMWF Seminar/Workshop on Interpretation of Numerical Weather Prediction Products*, 13–24 September 1982. ECMWF, Shinfield Park, Reading, UK., 161–206.

Hansen, A. R. 1986. Observational characteristics of atmospheric planetary waves with bimodal amplitude distribution. *Advances in Geophysics 29*, 101–133.

Hansen, A. R. and Chen, T. C. 1982. A spectral energetics analysis of atmospheric blocking. *Mon. Wea. Rev. 110*, 1146–1165.

Hansen, A. R. and Sutera, A. 1986. On the probability density distribution of planetary-scale atmospheric wave amplitude. *J. Atmos. Sci. 43*, 3250–3265.

Hollingsworth, A., Arpe, K., Tiedtke, M., Capaldo, M. and Savijarvi, H. 1980. The performance of a medium-range forecast model, in winter—impact of physical parameterizations. *Mon. Wea. Rev. 108*, 1736–1773.

Hollingsworth, A., Cubasch, U., Tibaldi, S., Brankovic, C., Palmer, T. N. and Campbell, L. 1987. Mid-latitude atmospheric prediction on time scales of 10–30 days. In: *Atmospheric and oceanic variability* (ed. H. Cattle.) Bracknell: Royal Meteorological Society, 117–151.

Hoskins, B. J. and Sardeshmukh, P. D. 1987. A diagnostic study of the dynamics of the northern hemisphere winter of 1985/86. *Q. J. R. Meteorol. Soc. 113*, 759–778.

Illari, L. and Marshall, J. C. 1983. On the interpretation of eddy fluxes during a blocking episode. *J. Atmos. Sci. 40*, 2232–2242.

Ji, L. R. and Tibaldi, S. 1983. Numerical simulations of a case of blocking: The effects of orography and land-sea contrast. *Mon. Wea. Rev. 111*, 2068–2086.

Källén, E. 1982. Bifurcation properties of quasi-geostrophic, barotrophic models and their relation to atmospheric blocking. *Tellus 34*, 255–265.

Lau, N.-C. 1983. Mid-latitude wintertime circulation anomalies appearing in a 15-year GCM experiment. In: *Large-scale dynamical processes in the atmosphere* (eds. B. J. Hoskins and R. P. Pearce.) New York: Academic Press, 111–125.

Lejenäs, H. and Döös, B. R. 1987. The behaviour of the stationary and travelling planetary-scale waves during blocking. A northern hemisphere data study. *J. Meteor. Soc. Japan 65*, 709–725.

Lejenäs, H. and Økland, H. 1983. Characteristics of Northern Hemisphere blocking as determined from a long time series of observational data. *Tellus 35A*, 350–362.

Lorenz, E. 1982. Atmospheric predictability experiments with a large numerical model. *Tellus 34*, 505–513.

Malguzzi, P. and Speranza, A. 1981. Local multiple equilibria and regional atmospheric blocking. *J. Atmos. Sci. 38*, 1939–1948.

Mansfield, D. A. 1984. The incidence of blocking in the Meteorological Office 5-level model. *Met. 013 Branch Memo. No. 99*. Available from U.K. Meteorological Office, Bracknell.

Molteni, F., Sutera, A. and Tronci, N. 1988. The EOFs of the geopotential eddies at 500 mb in winter and their probability density distributions. *J. Atmos. Sci. 45*, 3063–3080.

Palmer, T. N., Shutts, G. J. and Swinbank, R. 1986. Alleviation of a systematic westerly bias in general circulation and numerical weather prediction models through an orographic gravity wave drag parametrization. *Q. J. R. Meteorol. Soc. 112*, 1001–1039.

Rex, D. R. 1950. Blocking action in the middle troposphere and its effect upon regional climate. II: The climatology of blocking actions. *Tellus 2*, 275–302.

Shutts, G. J. 1986. A case study of eddy forcing during and Atlantic blocking episode. *Advances in Geophysics 29*, 135–164.

Speranza, A. 1986. Deterministic and statistical properties of northern hemisphere middle latitude circulation: minimal theoretical models. *Advances in Geophysics 29*, 199–266.

Sutera, A. 1986. Probability density distribution of large scale atmospheric flow. *Advances in Geophysics 29*, 319–338.

Tibaldi, S. 1986. Envelope orography and maintenance of the quasi-stationary circulation in the ECMWF global models. *Advances in Geophysics 29*, 339–374.

Tibaldi, S. and Ji, L. R. 1983. On the effect of model resolution on numerical simulation of blocking. *Tellus 35A*, 28–38.

Tibaldi, S., Brankovic, C. and Cubasch, U. 1987. 30-day integrations using the operational ECMWF spectral model. *ECMWF Tech. Memo. No. 138*. Available from ECMWF, Reading.

Wallace, J. M. and Gutzler, D. S. 1981. Teleconnections in the geopotential height field during the northern hemisphere winter. *Mon. Wea. Rev. 109*, 784–812.

Wallace, J. M., Tibaldi, S. and Simmons, A. J. 1983. Reduction of systematic forecast errors in the ECMWF model through the introduction of an envelope orography. *Q. J. R. Meteorol. Soc. 109*, 683–717.